International Journal of Thermophysics, Vol. 6, No. 2, 1985

Automated Differential Scanning Calorimetry at Low Temperatures

Å. Fransson[1] and G. Bäckström[1]

Received September 27, 1984

A Perkin–Elmer DSC-2 scanning calorimeter was operated by means of a PDP-11/34 computer with time-shared scanner and voltmeter. Special attention was paid to the problems of measurement below room temperature down to the low-temperature limit. It was found that Ne, rather than He, should be used as a purge gas, that scans should always be started at a standardized liquid nitrogen level, and that gas flow to the dry box should be stopped during measurements. Results on benzoic acid were then accurate to 0.6% from 120 to 300 K. The specific heat of antimony was measured in the temperature interval 120–720 K.

KEY WORDS: antimony; calorimetry; differential scanning calorimetry; low temperature; specific heat.

1. INTRODUCTION

A differential scanning calorimeter (DSC) measures the rates of heat absorption ($\dot{H}$) in two similar calorimeter vessels and outputs a signal proportional to the difference ($\Delta\dot{H}$) of these rates. A feedback mechanism keeps both calorimeters at closely the same temperature (T), which may be varied linearly as a function of time. Commercially available DSC instruments output two analogue signals corresponding to T and $\Delta\dot{H}$.

In recent years computer interfacing of DSC instruments has become frequent. Since computers are powerful tools both in data sampling systems and in data analysis, their use may be expected to improve the accuracy of DSC measurements. Mraw and Naas [1] reported molar heat capacities (C_p) with an error of 1–2% in the temperature range 250–700 K from

[1] Department of Physics, University of Umeå, S-901 87 Umeå, Sweden.

0195-928X/85/0300-0165$04.50/0

measurements with their Perkin–Elmer DSC-2 instrument, equipped with a Tektronix desk calculator. In the low-temperature range (100–250 K) and at the highest temperatures, however, the error given was 2–3 %.

In this paper we discuss problems concerning low-temperature measurements of c_p using a Perkin–Elmer DSC-2 instrument. We describe the interfacing with our PDP-11/34 computer and the software used to optimize measurements. Some important issues are the cooling effect of liquid nitrogen, the temperature gradients in the specimen, and the choice of calorimeter gas.

2. MEASUREMENT AND PROGRAMMING

The analogue outputs, U_T and U_H, from the Perkin–Elmer DSC-2 calorimeter are arranged to be linear functions of T and $\Delta\dot{H}$, respectively. We connected these output signals to a Hewlett–Packard 3456A digital voltmeter via an HP 3495A input multiplexer. Both units communicate with a PDP-11/34 computer via an IEEE 488 bus. By programming we achieve multiuser access to the voltmeter, the system being sufficiently fast to handle other experiments while DSC recordings are being made. On–off commands to the calorimeter are sent via an actuator card in the multiplexer box. The time in units of 0.01 s is obtained from the computer clock for each voltage measurement.

The output voltage, U_T, is converted to absolute temperature, T, using the following calibration procedure. We record the enthalpy peaks corresponding to the melting points in 1-hexene (99.9 % purity, Fluka, BRD), *n*-octane (99.8 %, Fluka), cyclohexane (99.95 %, BHD Chemicals, Great Britain), and indium (temperature standard provided by Perkin–Elmer) with transition temperatures of 133.38, 216.4, 279.75, and 429.78 K, respectively. When the values of U_T at incipient melting are determined, we fit a linear function, $T = A + BU_T$ to the resulting four data pairs. The constants A and B are determined at all scanning rates used. The resulting maximum deviation of the fits is generally 0.2 K at the lowest heating rate (0.31 $K \cdot min^{-1}$) and 2 K at 160 $K \cdot min^{-1}$.

The measuring procedure is similar in several respects to that described by Mraw and Naas [1]. For the first scan we place a standard specimen in the left calorimeter and an empty sample capsule in the other one. Keeping the temperature constant at its initial (i), static value, we determine the average U_T ($= U_{Ti}$) and U_H ($= U_{Hi}$). Dynamic values of U_T and U_H are then recorded, while T varies linearly with time up to the final value chosen. At the final (f) temperature we make another series of static (isothermal) measurements of U_T ($= U_{Tf}$) and U_H ($= U_{Hf}$). For the second scan we replace the standard specimen with an empty capsule and take

static, dynamic, and static data as before. For the third scan we place the specimen under investigation in the left calorimeter and repeat the same sequence of measurements. The above three scans use the same nominal values of $\dot{T}$ ($=dT/dt$) and U_H sensitivity. In order to reduce instrumental drift we complete the series of three scans in as short a time as possible. During c_p experiments T is measured versus time, and a third-order polynomial fitted to these data. The derivative of this polynomial yields the actual heating rate ($\dot{T}$).

As standard material for c_p we use aluminum oxide, the heat capacity of which is known to within 0.2% [2]. In order to take the small mass difference of the capsules into account, we use specific heat values for pure Al [3]. All weighing is done with a Sauter microbalance with a resolution of 10 μg.

The following are the main features of our Fortran program for measurement, preprocessing, and storage of data. The program is similar for each of the three scans.

Start.
Select temperature rate and time interval between measurements.
Do 15 static measurements of T_i and U_{Hi}.
Calculate averages of T_i and U_{Hi}.
Start the scan.
    Repeat dynamic measurements of T, U_H, and times until T becomes constant.
Wait for a fixed time to reach an equilibrium value of U_H.
Do 15 static measurements of T_f and U_{Hf}.
Calculate averages of T_f and static U_{Hf}.
Interpolate U_{Hi} and U_{Hf} to obtain signal U_{H0} from T_i to T_f.
Subtract static U_{H0} from dynamic U_H to obtain net U_H.
Store values of T, time, and net U_H in file.
End.

Any signal U_H may be written as follows:

$$U_H = U_0(t) + A\left\{\dot{T}\left[\Delta m_c c_c(T) + \sum_R mc - \sum_L mc\right] + \Delta P(T)\right\} \qquad (1)$$

where $U_0(t)$ = the amplifier output for zero input versus time, A = the amplification factor for U_H, $\dot{T}$ = the actual temperature rate, Δm_c = the difference in mass between calorimeters, $c_c(T)$ = the specific heat capacity of calorimeter material (Pt-Ir), $\sum mc$ = the sum over heat capacities in the left (L) or right (R) calorimeter, and $\Delta P(T)$ = the difference in power loss by

conduction and radiation from calorimeter vessels (including instrumental terms).

The amplification factor, A, is assumed to be independent of time, since its constancy may be assured by feedback. The power loss difference, $\Delta P(T)$, is taken to be a function of T only, although it depends on other factors, which we attempt to keep constant. Using Eq. (1) we may now obtain an expression for U_{H0},

$$U_{H0} = U_0(t) + A\Delta P(T) \tag{2}$$

Subtracting U_{H0} from U_{H1}, which is obtained in the first scan with a standard (reference) specimen (r) in the left calorimeter, we have

$$U_1 \equiv U_{H1} - U_{H0} = A\dot{T}_1(\Delta m_c c_c + m_r c_r + \Delta_1 m_p c_p) \tag{3}$$

where the subscript r refers to the reference and p to the Al capsules (pans). We have taken $U_0(t) - U_0(t_0)$ to be zero, although this difference may fluctuate. Similarly we obtain for the second and third scans

$$U_2 \equiv U_{H2} - U_{H0} = A\dot{T}_2(\Delta m_c c_c + \Delta_2 m_p c_p) \tag{4}$$

$$U_3 \equiv U_{H3} - U_{H0} = A\dot{T}_3(\Delta m_c c_c + m_s c_s + \Delta_3 m_p c_p) \tag{5}$$

Dividing by the temperature rate and subtracting pairs of equations, we then obtain

$$\begin{aligned} U_1/\dot{T}_1 - U_2/\dot{T}_2 &= A(m_r c_r + \Delta_1 m_p c_p - \Delta_2 m_p c_p) \\ U_3/\dot{T}_3 - U_2/\dot{T}_2 &= A(m_s c_s + \Delta_3 m_p c_p - \Delta_2 m_p c_p) \end{aligned} \tag{6}$$

Eliminating A we immediately have an expression for the specific heat capacity, c_s.

Our instrument is equipped with a "factory second" calorimeter head, which according to Perkin–Elmer has not been tested in the low-T range and therefore cannot be guaranteed to yield a flat variation of $\Delta P(T)$. However, since $\Delta P(T)$ is eliminated in the above analysis, its flatness should be irrelevant to the extent that $\Delta P(T)$ is equally large in the three related scans. An important detail in this respect is the angular orientation of the calorimeter covers, which according to our experience does influence $\Delta P(T)$. We therefore always use the same orientation in a sequence of three scans.

The difference between the static signals U_{Hi} and U_{Hf} may be reduced by time-consuming electronic adjustments but cannot be permanently eliminated. However, in the calculation of the specific heat capacity (c_p), the temperature variation of the static signal becomes unimportant, since

the $A\Delta P(T)$ terms cancel in Eqs. (3)–(5). The static signal can be measured only before and after a scan. We arbitrarily make a linear interpolation between U_{Hi} and U_{Hf} to obtain the static signal, U_{H0} versus T. When we subtract these static values from the measured U_H, we find the reproducibility of $U_H - U_{H0}$ to be within 0.5%, even when the difference $U_{Hf} - U_{Hi}$ varies by as much as 25% of the net signal $U_H - U_{H0}$ between scans. This high reproducibility shows that the time dependence of $U_0(t)$ is small.

The sample holder is purged with a dry gas to prevent condensation, create a constant temperature environment, and remove any gas emitted from the sample. We have tried using pure neon as an alternative to helium in connection with liquid nitrogen cooling. Helium, having a higher thermal conductivity, permits a higher cooling rate and decreases the transient on going from the scanning to the static mode. Neon, on the other hand, should decrease the magnitude of $\Delta P(T)$ on account of its lower thermal conductivity and may thus be expected to reduce the change of $\Delta P(T)$ between scans.

The heat loss term, $\Delta P(T)$, is also determined by the difference between the temperature of the calorimeter vessels and that of the surrounding calorimeter block. A small temperature difference implies a small $\Delta P(T)$, which is desirable from the point of view of accuracy, but it also reduces the attainable cooling rate, so a compromise must be found in each case. In our system we cool either by means of a heat pump (Perkin–Elmer Intracooler II) or by a tank containing liquid nitrogen. Sources of error arising because of the cooling with liquid nitrogen are discussed in the next section.

3. ERRORS

Appreciable temperature gradients may be produced in a sample of low thermal diffusivity. The measured heat capacity values will thus become too low or too high, depending on the values of $\partial c_p/\partial T$ for sample and reference material. It would be tempting to take mean values of results from heating and cooling scans, but undercooling would make temperature calibration unreliable in the latter case. Suitable second-order phase transitions would have to be found for this application. Many order–disorder, ferroelectric, antiferroelectric, and antiferromagnetic transitions are in fact available in the range 100–300 K.

Mraw and Naas [1] noted that a combination of liquid nitrogen cooling and helium purge gas caused distortion of the melting peaks, especially at a low scanning rate. However, they did not attempt to account for this phenomenon. We have observed that In melting peaks indeed become dis-

torted when He gas is used (Fig. 1, curve A), compared to the peak obtained under similar conditions (0.31 $K \cdot min^{-1}$) in Ne gas (curve D). The integrals over these enthalpy peaks were, however, not significantly different. The comparison was made using standard Al sample capsules. When gas-tight Al capsules were used with He gas, the shape became almost normal (curve B), although some distortion remained. The peak was much less affected by the use of a gas-tight capsule in the case of Ne (curve C). The difference between curve C and curve D may be accounted for by a change in sample mass and the associated time delay.

As shown in Fig. 2, our measured values of c_p for benzoic acid (NBS standard, 99.99%) are lower when He is used as a purge gas. The deviation of our smoothed data from those reported by Ginnings and Furukawa [2] is -2.0 to -1.5% from 120 to 300 K. With Ne the deviation is reduced to 0.6% or less (Fig. 2, curve A). Neon purge gas reduced the scatter in the measured data by one fourth to 1% or less (Fig. 3) and completely

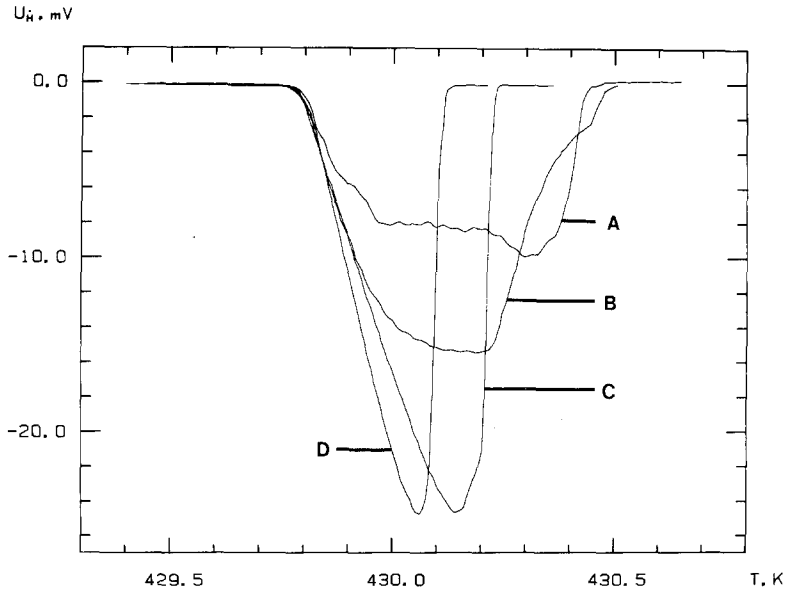

Fig. 1. Melting peaks of indium at 0.31 $K \cdot min^{-1}$. The peaks have been adjusted in temperature for easier comparison. Purge-gas pressure, 0.21 MPa throughout. (A) Standard Al capsule; He purge gas; sample mass, 6.37 mg; enthalpy signal sensitivity $R = 2.1\ mJ \cdot s^{-1}$. (B) Gas-tight Al capsule; He purge gas; sample mass, 17.97 mg; $R = 4.2\ mJ \cdot s^{-1}$. (C) Gas-tight Al capsule; Ne purge gas; sample mass, 17.97 mg; $R = 4.2\ mJ \cdot s^{-1}$. (D) Standard Al capsule; Ne purge gas; sample mass, 6.37 mg; $R = 2.1\ mJ \cdot s^{-1}$.

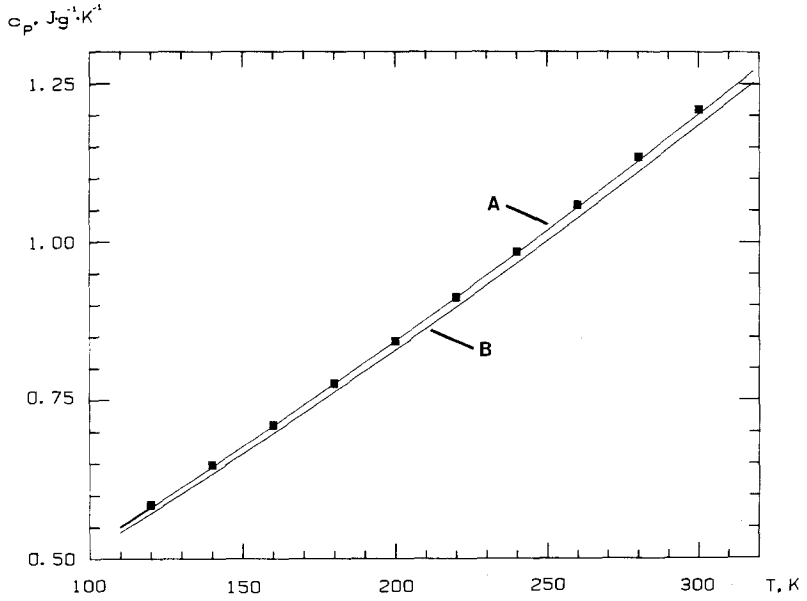

Fig. 2. Specific heat of benzoic acid versus temperature. (Curve A) Our smoothed results; neon purge gas at 0.21 MPa. (Curve B) Our smoothed results; helium purge gas at 0.21 MPa. (■) Adiabatic results by Ginnings and Furukawa [2].

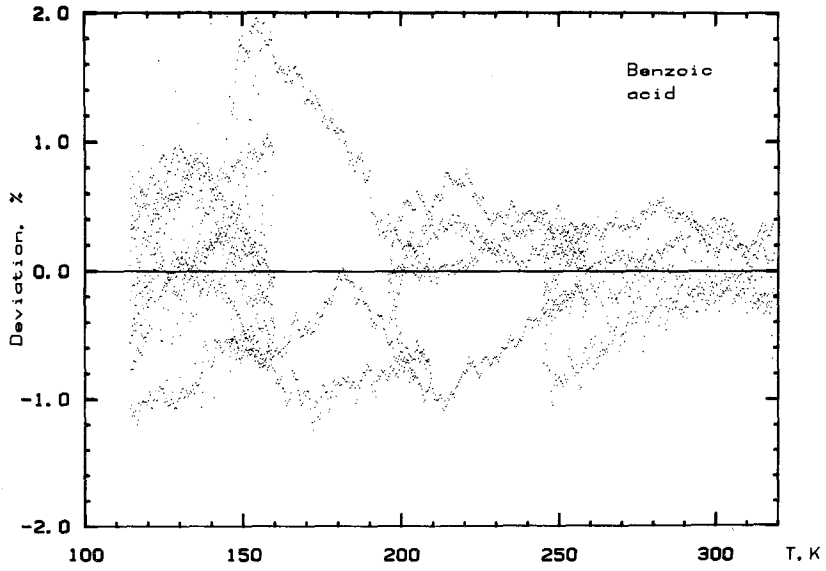

Fig. 3. Deviation of experimental data from curve A, Fig. 2, versus temperature. Neon purge gas at 0.21 MPa.

eliminated distortions of the melting peaks. The fact that peak distortion was alleviated by the use of gas-tight capsules might be taken to indicate that the presence of He in the sample capsule is the key factor. A solution of He in In would in fact exhibit a melting range. However, although He is known to diffuse readily through most metals, its solubility is presumably too small to result in a measurable melting range. In addition, we do not find indications of a heat of solution, since the enthalpy per unit mass is the same for all the peaks in Fig. 1.

The normal sample capsule also differs from the gas-tight variety by having a larger base area. This property may produce distorted, wide peaks by the following mechanism. The Pt–Ir calorimeter vessels are heated by strips in contact with the bottoms, and the resistance thermometers are similarly attached. Detailed information about sizes and positions of these components does not seem to be available in the literature. The vessels are, however, heated over part of the bottom, whereas cooling takes place over all of the outer surface. Temperature gradients are thus produced in the vessel, and due to the high thermal conductivity of the He gas, these gradients are expected to be about three times larger than in the case of Ne. The sample capsule is thermally coupled to the vessel by the flow gas but probably mainly by direct contact between the metallic surfaces. Depending on the detailed forms of these surfaces, intimate contact will occur over one or three smaller areas. A specimen in its solid state will similarly contact one or three spots at the bottom of the sample capsule. On melting, the contact areas will increase and in general move along the bottom of the capsule. In view of the appreciable thermal gradients existing with He as a flow gas, this change in the conditions of contact may well lead to irregularities of the melting peak. Analogously we interprete the different results shown in Fig. 2 as a change in temperature drop of about 3 K between the thermometer and the sample. We thus agree with Mraw and Naas [1] in their recommendation that He should be avoided as a flow gas at low temperatures. If our interpretation is correct, their mixed flow gas, containing 10% He, should also be acceptable.

Variations in excess pressure (or gas flow rate) could influence measured values. However, experiments that we carried out at Ne gas pressures of 0.07, 0.14, 0.21, and 0.28 MPa gave no detectable effect on the baseline (U_2) in the range 115–190 K. On the other hand, increased overpressure enhances the heat exchange between the purge gas and the calorimeter vessels. As a consequence the transient on switching from the scanning (U_H) to the static mode (U_{H0}) is shortened. We found that increasing the excess pressure from 0.14 to 0.21 MPa at 115 K decreased the duration of the transient from 3 to 1 min. Further increase in gas pressure is expected eventually to increase the scatter of measured data.

The manufacturer of the DSC-2 recommends the use of a constant flow of dried gas through the antifrost box during operation at low tempratures. A small excess pressure in this box prevents back diffusion of humid air. However, we have found the heat signal to be sensitive to pressure changes in the dry box. When we replaced a damaged O-ring in the calorimeter holder assembly, the sensitivity to pressure was reduced but not completely eliminated. The pressure in the box is in fact far from constant in spite of the regulating valve provided by the manufacturer. We solved this problem by completely stopping the gas flow through the dry box during scans.

The instrument is provided with a reservoir for liquid nitrogen cooling of the calorimeter block. We have noticed that the heat signal depends, dynamically as well as statically, on the nitrogen level in the tank. Variation in this level was in fact found to be responsible for the major part of the scatter in the DSC scans. Cowie et al. [4] also mention similar effects. In order to improve accuracy, we start scans with a half-filled reservoir and limit the temperature range of each scan at about 70 K. We have tested this procedure on benzoic acid in the range 110–320 K, using a heating rate of $10\,\mathrm{K}\cdot\mathrm{min}^{-1}$ and a purge-gas pressure of 0.14 MPa. Two series of measurements were taken, one with an uncontrolled nitrogen level and one with a half-filled tank. The scatter of the specific heat values proved to be only one half in the latter case.

4. RESULTS AND DISCUSSION

We first tested our procedures on a sample (NBS standard) of benzoic acid. Eight independent measurements were performed in the lowest temperature interval, 110–160 K, three between 140 and 210 K, and four in the remaining temperature intervals. The experimental scatter was constant, $\sigma = 0.006\,\mathrm{J}\cdot\mathrm{g}^{-1}\cdot\mathrm{K}^{-1}$, in all intervals measured. As shown in Fig. 2, curve A, our averaged data are in excellent agreement with values from adiabatic calorimetry.

As an additional project we chose to study antimony (Fluka, BRD, 99.9999%), since no recommended values are given for 70–587 K in the compilation by Touloukian and Buyco [5]. The reason may have been doubtful sample purity in previous experiments or possibly a large discrepancy among published results. Figure 4 shows our mean values of c_p as well as a representation by a smoothed curve. Our results between 120 and 720 K can be summarized, with a standard deviation of 0.7%, by the equation

$$c_p = 0.1941 + 5.09 \times 10^{-5} T - 161.5/(T^2 - 7655) \qquad (7)$$

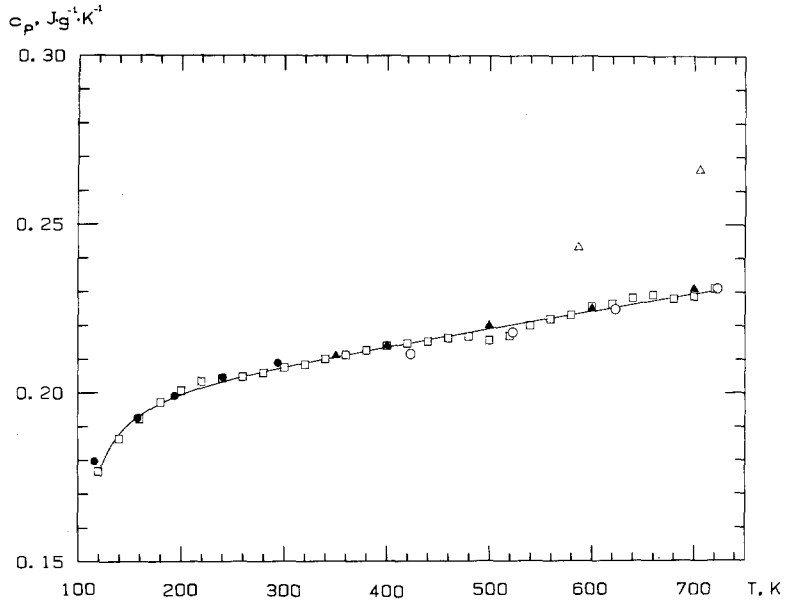

Fig. 4. Specific heat of antimony versus temperature. (□) Mean values from this work; (●) Jaeger et al. from Touloukian and Buyco [5]; (▲) Kramer and Nölting [6]; (○) Umino [7]; (△) Kochetkova and Rezukhina from Touloukian and Buyco [5]; (——) Eq. (7), fitted to the man values of this work.

Table I. Specific Heat of Antimony According to Eq. (7)

T (K)	c_p (J·g^{-1}·K^{-1})
120	0.176
160	0.193
200	0.199
240	0.203
280	0.206
320	0.209
360	0.211
400	0.213
440	0.216
480	0.218
520	0.220
560	0.222
600	0.224
640	0.226
680	0.228
720	0.230

where c_p is in $J \cdot g^{-1} \cdot K^{-1}$ and T is in K. Values of c_p for Sb according to Eq. (7) are given in Table I. The smoothed data agree very well with other published results, with the exception of those by Kochetkova and Rezukhina [5], as may be seen from Fig. 4. Some deviation from earlier values may also be noticed at the low temperature end, our values being lower by 3.5% than those of Jaeger et al. [5]. Above 700 K the specific heat values gradually became time dependent, possibly due to vacancy formation.

ACKNOWLEDGMENT

This work was financially supported by the Swedish Natural Science Research Council.

REFERENCES

1. S. C. Mraw and D. F. Naas, *J. Chem. Thermodyn.* **11**:567 (1979).
2. D. C. Ginnings and G. T. Furukawa, *J. Am. Chem. Soc.* **75**:522 (1953).
3. Y. S. Touloukian and E. H. Buyco, *Thermophysical Properties of Matter* (Plenum, New York, 1970), Vol. 4, pp. 1–5.
4. J. M. G. Cowie, I. J. McEwen, and M. Y. Pedram, *Macromolecules* **16**:1151 (1983).
5. Y. S. Touloukian and E. H. Buyco, *Thermophysical Properties of Matter* (Plenum, New York, 1970), Vol. 4, pp. 6–8.
6. W. Kramer and J. Nölting, *Acta Metall.* **20**:1353 (1972).
7. S. Umino, *Sci. Rep. Tohoku Impl. Univ.* **15**(Ser. 1):597 (1926).